

---

# Mapping Images to Scene Graphs with Permutation-Invariant Structured Prediction

---

Roei Herzig<sup>\*1</sup> Moshiko Raboh<sup>\*1</sup> Gal Chechik<sup>2,3</sup> Jonathan Berant<sup>1</sup> Amir Globerson<sup>1</sup>

## Abstract

Structured prediction is concerned with predicting multiple inter-dependent labels simultaneously. Classical methods like CRF achieve this by maximizing a score function over the set of possible label assignments. Recent extensions use neural networks to either implement the score function or in maximization. The current paper takes an alternative approach, using a neural network to generate the structured output directly, without going through a score function. We take an axiomatic perspective to derive the desired properties and invariances of a such network to certain input permutations, presenting a structural characterization that is provably both necessary and sufficient. We then discuss graph-permutation invariant (GPI) architectures that satisfy this characterization and explain how they can be used for deep structured prediction. We evaluate our approach on the challenging problem of inferring a *scene graph* from an image, namely, predicting entities and their relations in the image. We obtain state-of-the-art results on the challenging Visual Genome benchmark, outperforming all recent approaches.

## 1. Introduction

Structured prediction addresses the problem of classification when the label space contains multiple inter-dependent labels. For example, in semantic segmentation of an image, each pixel is assigned a label, while considering the labels of nearby pixels. A similar problem is the task of recognizing multiple entities and their relations in an image, where recognizing one entity affects recognition of the others. Structured prediction has attracted considerable attention because it applies to many learning problems and poses unique theoretical and applied challenges (e.g., see Taskar et al., 2004; Chen et al., 2015; Belanger et al., 2017).

<sup>\*</sup>Equal contribution <sup>1</sup>Tel-Aviv University, Israel <sup>2</sup>Google Brain, CA, 94043 <sup>3</sup>Gonda brain research institute, Bar-Ilan University, Ramat-Gen 52900, Israel. Correspondence to: Roei Herzig <roei-herzig@tau.ac.il>, Moshiko Raboh <shikorab@gmail.com>, Gal Chechik <gal.chechik@gmail.com>, Jonathan Berant <joberant@cs.tau.ac.il>, Amir Globerson <amir.globerson@tau.ac.il>.

Typically, structured prediction models define a score function  $s(x, y)$  that quantifies how well a label assignment  $y$  is compatible, or consistent, with an input  $x$ . In this setup, the *inference task* amounts to finding the label that maximizes the compatibility score  $y^* = \arg \max_y s(x, y)$ . This score-based approach separates a scoring component – implemented by a parametric model, from an optimization component – aimed at finding a label that maximizes that score. Unfortunately, for a general scoring function  $s(\cdot)$ , the space of possible label assignments grows exponentially with input size. For instance, the set of possible pixel label assignments is too large even for small images. Thus, inferring the label assignment that maximizes a scoring function is computationally hard in the general case.

An alternative approach to scored-based methods is to map an input  $x$  to a structured output  $y$  with a “black box” neural network, without explicitly defining a score function. This raises a natural question: what properties and invariances must be satisfied by such a network? We take this axiomatic approach and argue that one important property is invariance to a particular type of input permutation. We then prove that this invariance is equivalent to imposing certain structural constraints on the architecture of the network, and describe architectures that satisfy these constraints, significantly extending the expressive power of current structured prediction approaches. We argue that respecting permutation invariance is important, as otherwise the model would have to spend capacity on learning this invariance at training time. Conceptually, our approach is motivated by recent work on DEEPSSETS (Zaheer et al., 2017), which asked a similar question for black-box functions on sets.

To evaluate our approach, we tackle the challenging task of mapping an image to a *scene graph*, which describes the entities in the image and their relations. We describe a model that satisfies the permutation invariance property, and show that it achieves state-of-the-art results on the competitive Visual Genome benchmark (Krishna et al., 2017), demonstrating the power of our new design principle.

In summary, the novel contributions of this paper are: First, we derive sufficient and necessary conditions for a deep structured prediction architecture. Second, we improve the state-of-the-art with this approach in a challenging pixel-to-graph problem on a large dataset of complex visual scenes.

## 2. Structured Prediction

Score-based methods in structured prediction define a score function  $s(x, y)$ <sup>1</sup> that reflects the degree to which  $y$  is compatible with  $x$ , and infer a label by solving  $y^* = \arg \max_y s(x, y)$  (e.g., see Lafferty et al., 2001; Taskar et al., 2004; Meshi et al., 2010; Chen et al., 2015; Belanger et al., 2017). Most score functions previously used decompose as a sum over *simpler* functions,  $s(x, y) = \sum_i f_i(x, y)$ , where solving  $\max_y f_i(x, y)$  can be performed efficiently.<sup>2</sup> This local maximization forms the basic building block of algorithms for approximately maximizing  $s(x, y)$ . One way to achieve this is to restrict  $f_i(x, y)$  to depend only on a small subset of the  $y$  variables.

The renewed interest in deep learning led to efforts to integrate deep networks with structured prediction, including modeling the  $f_i$  functions as deep networks. In this context, the most widely-used score functions are singleton  $f(y_i, x)$  and pairwise  $f_{ij}(y_i, y_j, x)$ . Initial work used a two-stage architecture, learning local scores independently of the structured prediction goal (Chen et al., 2014; Farabet et al., 2013). Later works considered *end-to-end* architectures where the inference algorithm is part of the computation graph (Chen et al., 2015; Pei et al., 2015; Schwing & Urtasun, 2015; Zheng et al., 2015). These studies used standard inference algorithms, such as loopy belief propagation, mean field methods and gradient descent (Belanger et al., 2017).

Score-based methods provide several advantages. First, they allow intuitive specification of local dependencies between labels (like pairwise dependencies) and how these translate to global dependencies. Second, when the score function is linear in its parameters ( $s(x, y; \mathbf{w})$  is linear in  $\mathbf{w}$ ), the learning problem has natural convex surrogates (e.g., log-loss in CRF), making learning efficient. Third, inference in large label spaces is often possible via exact combinatorial algorithms or empirically accurate approximations.

However, with the advent of deep scoring functions  $s(x, y; \mathbf{w})$ , learning is no longer convex. Thus, it is worthwhile to rethink the architecture of structured prediction models, and consider models that map inputs  $x$  to outputs  $y$  directly without an explicit score function. We want these models to enjoy the expressivity and predictive power of neural networks, while maintaining the ability to specify local dependencies between labels in a flexible manner. In the next section, we present such an approach and consider a natural question: what should be the properties of such a deep neural network used for structured prediction.

<sup>1</sup>The term energy function is also used.

<sup>2</sup>More precisely, many message passing algorithms require that functions  $f_i(x, y) + \sum_k \delta_k(y_k)$  can be maximized efficiently.

## 3. Permutation Invariant Structured Prediction

We begin with some notation, focusing on structures that consists of pairwise interactions, as these are simpler in terms of notation, and sufficient for describing the structure in many problems.

We denote a structured label with  $n$  entries by  $y = [y_1, \dots, y_n]$ . In a score-based approach, the score is defined via a set of singleton scores  $f_i(y_i, x)$  and pairwise scores  $f_{ij}(y_i, y_j, x)$ , where the overall score  $s(x, y)$  is the sum of these singleton and pair scores. For brevity, we also denote  $f_{ij} = f_{ij}(y_i, y_j, x)$  and  $f_i = f_i(y_i, x)$ . An inference algorithm takes as input the set of local scores  $f_i, f_{ij}$  and outputs the assignment maximizing  $s(x, y)$ . We can therefore abstractly view an inference algorithm as a black-box that takes as input a set of node- and edge-dependent inputs (i.e., the local scores  $f_i, f_{ij}$ ) and returns a label  $y$ , even without an explicit score function  $s(x, y)$ . While numerous inference algorithms exist for this setup, including belief propagation (BP) and mean field, here we aim to develop a framework for a deep learning labeling algorithm (we avoid the term ‘‘inference’’ since the algorithm does not explicitly maximize a score function). Such an algorithm will be a black-box with the  $f$  functions as input and the labels  $y_1, \dots, y_n$  as output. We next ask what architecture such an algorithm should have.

We follow with several definitions. A *graph labeling function*  $\mathcal{F} : (V, E) \rightarrow Y$  is a function whose input is an ordered set of node features  $V = [z_1, \dots, z_n]$  and ordered set of edge features  $E = [z_{1,2}, \dots, z_{i,j}, \dots, z_{n,n-1}]$ . For example, the  $z_i$ ’s can be the array of values  $f_i(y_i, x)$ , and the  $z_{i,j}$ ’s can be the table of values  $f_{i,j}(y_i, y_j, x)$ . For simplicity, assume  $z_i \in \mathbb{R}^d$  and  $z_{i,j} \in \mathbb{R}^e$ . The output of  $\mathcal{F}$  is a set of labels  $\mathbf{y} = [y_1, \dots, y_n]$ , which can be thought of as labeling the nodes. Thus, inference algorithms like BP are graph labeling functions, since they take  $f$  as input and output a set of labels. However, graph labeling functions need not correspond to any inference algorithm (i.e., an algorithm that maximizes a score function).

A natural requirement is that the algorithm produces the same result when given the same score function. For example, consider a label space containing three variables  $y_1, y_2, y_3$ , and assume that the inference algorithm takes as input  $\mathbf{z} = (z_1, z_2, z_3, z_{12}, z_{13}, z_{23}) = (f_1, f_2, f_3, f_{12}, f_{13}, f_{23})$ , and outputs a label  $\mathbf{y} = (y_1^*, y_2^*, y_3^*)$ . When the same algorithm is given an input that is permuted in a consistent way,  $\mathbf{z}' = (f_2, f_1, f_3, f_{21}, f_{23}, f_{13})$ , this defines *exactly* the same score function as the first scenario. Hence, we would expect it to output the same label, only permuted, namely, it should output  $\mathbf{y} = (y_2^*, y_1^*, y_3^*)$ . Most inference algorithms, including BP and mean field, satisfy this symmetry requirement by de-

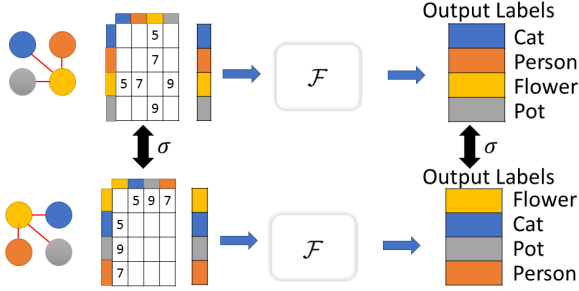


Figure 1. **Graph permutation invariance and structured prediction.** A graph labeling function  $\mathcal{F}$  is graph permutation invariant (GPI) if permuting the names of nodes maintains the output.

sign. Here we design a deep learning black-box, hence need to guarantee invariance to input permutations. A black-box that does not satisfy this invariance has to waste capacity on learning it at training time.

In what follows we use  $\mathbf{z}$  to denote the joint set of node and edge features.  $\mathbf{z}$  can be thought of as a container with  $n + n(n - 1) = n^2$  elements.

We next consider what happens to a graph labeling function, when graph variables are permuted by a permutation  $\sigma$ . Importantly, the edges in this case are also permuted in a way that is consistent with the node permutation  $\sigma$ .

**Definition 1.** Let  $\mathbf{z}$  be a set of node and edge features. Given a permutation  $\sigma$  of  $\{1, \dots, n\}$ , denote  $\sigma(\mathbf{z})$  to be a new set of node and edge features that are given by:

$$[\sigma(\mathbf{z})]_i = \mathbf{z}_{\sigma(i)} \quad , \quad [\sigma(\mathbf{z})]_{i,j} = \mathbf{z}_{\sigma(i),\sigma(j)}. \quad (1)$$

$\sigma(\mathbf{z})$  has the same elements as in  $\mathbf{z}$ , but the node elements are permuted according to  $\sigma$ , and the edge elements are permuted accordingly. In what follows, we use the notation  $\sigma([y_1, \dots, y_n]) = [y_{\sigma(1)}, \dots, y_{\sigma(n)}]$ , namely,  $\sigma$  applied to a set of labels yields the same labels, only permuted by  $\sigma$ . Next comes our key definition of a function  $\mathcal{F}$  whose output is invariant to permutations of the input graph.

**Definition 2.** A graph labeling function  $\mathcal{F}$  is said to be **graph-permutation invariant (GPI)**, if for all permutations  $\sigma$  of  $\{1, \dots, n\}$  and for all  $\mathbf{z}$  it satisfies:

$$\mathcal{F}(\sigma(\mathbf{z})) = \sigma(\mathcal{F}(\mathbf{z})). \quad (2)$$

Figure 1 illustrates the desired invariance. The above property says that as long as the input to  $\mathcal{F}$  describes the same node and edge properties, the same labeling will be output. This is indeed a property we would like any such  $\mathcal{F}$  to have, and we thus turn to characterizing a necessary and sufficient structure for achieving it.

### 3.1. Characterizing Permutation Invariance

Motivated by the above discussion, we ask: what structure is necessary and sufficient to guarantee that  $\mathcal{F}$  is graph-permutation invariant? Note that a function  $\mathcal{F}$  takes as input an **ordered** set  $\mathbf{z}$ . Therefore its output on  $\mathbf{z}$  could certainly differ from its output on  $\sigma(\mathbf{z})$ . To achieve permutation invariance,  $\mathcal{F}$  should intuitively contain certain symmetries. For example, one permutation invariant architecture is to define  $y_i = g(\mathbf{z}_i)$  for any function  $g$ , but this characterization is too restrictive to cover all permutation invariant functions. The next Theorem provides a complete characterization, while Figure 2 shows the corresponding architecture.

**Theorem 1.** Let  $\mathcal{F}$  be a graph labeling function. Then  $\mathcal{F}$  is graph-permutation invariant if and only if there exist functions  $\alpha, \rho, \phi$  such that for all  $k = 1, \dots, n$ :

$$[\mathcal{F}(\mathbf{z})]_k = \rho(\mathbf{z}_k, \sum_{i=1}^n \alpha(\mathbf{z}_i, \sum_{j \neq i} \phi(\mathbf{z}_i, \mathbf{z}_{i,j}, \mathbf{z}_j))), \quad (3)$$

where  $\phi : \mathbb{R}^{2d+e} \rightarrow \mathbb{R}^L$  and  $\alpha : \mathbb{R}^{d+L} \rightarrow \mathbb{R}^W$  and  $\rho : \mathbb{R}^{W+d} \rightarrow \mathbb{R}$ .

*Proof.* First, we show that any  $\mathcal{F}$  satisfying the conditions of Theorem 1 is GPI. Namely, for any permutation  $\sigma$ ,  $[\mathcal{F}(\sigma(\mathbf{z}))]_k = [\mathcal{F}(\mathbf{z})]_{\sigma(k)}$ . To see this, write  $[\mathcal{F}(\sigma(\mathbf{z}))]_k$  using Eq. 3 and Definition 1 as:

$$\rho(\mathbf{z}_{\sigma(k)}, \sum_i \alpha(\mathbf{z}_{\sigma(i)}, \sum_{j \neq i} \phi(\mathbf{z}_{\sigma(i)}, \mathbf{z}_{\sigma(i),\sigma(j)}, \mathbf{z}_{\sigma(j)})).$$

The second argument of  $\rho$  above is clearly invariant under  $\sigma$ , because the sum considers an index  $i$  and all other indices  $j$ , hence the same elements are covered under permutation. The expression therefore equals to:

$$\rho(\mathbf{z}_{\sigma(k)}, \sum_i \alpha(\mathbf{z}_i, \sum_{j \neq i} \phi(\mathbf{z}_i, \mathbf{z}_{i,j}, \mathbf{z}_j))) = [\mathcal{F}(\mathbf{z})]_{\sigma(k)}$$

where the equality follows from Eq. 3. We thus proved that Eq. 3 implies graph permutation invariance.

Next, we prove that any black-box graph-permutation invariant function can be expressed as in Eq. 3. Namely, we show how to define  $\phi, \alpha$  and  $\rho$  that can implement any permutation invariant function  $\mathcal{F}$ . The key idea is to construct  $\phi, \alpha$  such that the second argument of  $\rho$  in Eq. 3 contains all the information about the graph features  $\mathbf{z}$ , including the edges they originated from. Then, the function  $\rho$  consists of an application of the black box  $\mathcal{F}$  to this representation, followed by extracting the label  $y_k$ .

To simplify notation assume that edge features are scalar ( $e = 1$ ). The extension to the vector case is simple, but involves more indexing. We also assume that  $\mathbf{z}_k$  uniquely identifies the node (i.e., no two nodes share the same node

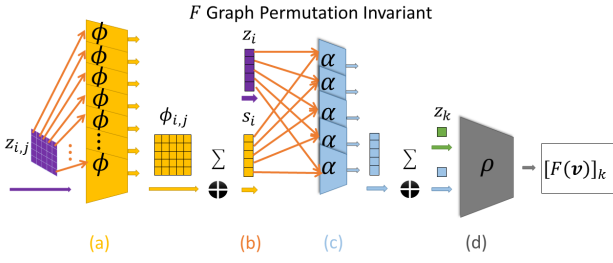


Figure 2. A schematic representation of the GPI architecture in Theorem 1. Singleton features  $z_i$  are omitted for simplicity. First, the features  $z_{i,j}$  are processed element-wise by  $\phi$ . Next, they are summed to create a vector  $s_i$ , which is concatenated with  $z_i$ . Third, a representation of the entire graph is created by applying  $\alpha$   $n$  times and summing the created vector. The graph representation is then finally processed by  $\rho$  together with  $z_k$ .

feature), which can be achieved by adding the index as another feature of  $z_k$ . Finally, we assume that  $\mathcal{F}$  is a function only of the pairwise features  $z_{i,j}$ . This can be achieved by adding singleton features into the pairwise ones.

Let  $H$  be a hash function with  $L$  buckets mapping node features  $z_i$  to an index (bucket). Assume that  $H$  is perfect (this can be achieved for a large enough  $L$ ). Define  $\phi$  to map the pairwise features to a vector of size  $L$ . Let  $\mathbb{1}[j]$  be a one-hot vector of dimension  $\mathbb{R}^L$ , with one in the  $j^{\text{th}}$  coordinate. Recall that we consider scalar  $z_{i,j}$  so that  $\phi$  is indeed in  $\mathbb{R}^L$ , and define  $\phi$  as:

$$\phi(z_i, z_{i,j}, z_j) = \mathbb{1}[H(z_j)] z_{i,j} \quad (4)$$

i.e.,  $\phi$  “stores”  $z_{i,j}$  in the unique bucket for node  $j$ .

Let  $s_i = \sum_{j \neq i} \phi(z_i, z_{i,j}, z_j)$  be the second argument of  $\alpha$  in Eq. 3 ( $s_i \in \mathbb{R}^L$ ). Then, since all  $z_j$  are distinct,  $s_i$  stores all the pairwise features for neighbors of  $i$  in unique positions within its  $L$  coordinates. Since  $s_i(H(z_k))$  contains the feature  $z_{i,k}$  whereas  $s_j(H(z_k))$  contains the feature  $z_{j,k}$ , we cannot simply sum the  $s_i$ , since we would lose the information of which edges the features originated from. Instead, we define  $\alpha$  to map  $s_i$  to  $\mathbb{R}^{L \times L}$  such that each feature is mapped to a distinct location. Formally:

$$\alpha(z_i, s_i) = \mathbb{1}[H(z_i)] s_i^T. \quad (5)$$

$\alpha$  outputs a matrix that is all zeros except for the features corresponding to node  $i$  that are stored in row  $H(z_i)$ . The matrix  $M = \sum_i \alpha(z_i, s_i)$  (namely, the second argument of  $\rho$  in Eq. 3) is a matrix with all the edge features in the graph including the graph structure.

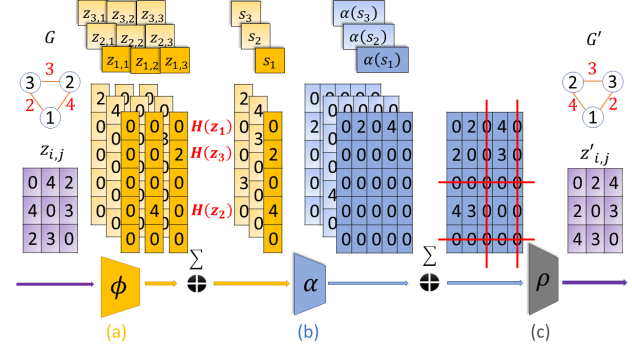


Figure 3. Illustration of the proof construction for Theorem 1. Here  $H$  is a hash function of size  $L = 5$  such that  $H(1) = 1, H(3) = 2, H(2) = 4$ ,  $G$  is a three-node input graph, and  $z_{i,j} \in \mathbb{R}$  are the pairwise features (in purple) of  $G$ . (a)  $\phi$  is applied to each  $z_{i,j}$ . Each application yields a vector in  $\mathbb{R}^5$ . The three dark yellow columns correspond to  $\phi(z_{1,1}), \phi(z_{1,2})$  and  $\phi(z_{1,3})$ . Then, all vectors  $\phi(z_{i,j})$  are summed over  $j$  to obtain three  $s_i$  vectors. (b)  $\alpha$ 's (blue matrices) are an outer product between  $\mathbb{1}[H(z_i)]$  and  $s_i$  (see Eq. 5) resulting in a matrix of zeros except one row. The dark blue matrix corresponds for  $\alpha(z_1, s_1)$ . (c) All  $\alpha$ 's are summed to a  $5 \times 5$  matrix, isomorphic to the original  $z_{i,j}$  matrix.

To complete the construction we set  $\rho$  to have the same outcome as  $\mathcal{F}$ . We first discard rows and columns in  $M$  that do not correspond to original nodes (reducing  $M$  to dimension  $n \times n$ ). Then, we use the reduced matrix as the input  $z$  to the given  $\mathcal{F}$ . Assume for simplicity that  $M$  does not need to be contracted.<sup>3</sup> Let the output of  $\mathcal{F}$  on  $M$  be  $\mathbf{y} = y_1, \dots, y_n$ . Then we set  $\rho(z_k, M) = \mathbf{y}_{H(z_k)}$ . Since  $\mathcal{F}$  is invariant to permutations this indeed returns the output of  $\mathcal{F}$  on the original input.  $\square$

**General Graphs** So far, we discussed complete graphs, where all edges correspond to valid feature pairs. Many graphs however may be sparse and have certain structures. For example, an  $n$ -variable chain graph in sequence labeling has only  $n - 1$  edges. For such sparse graphs, the input to  $\mathcal{F}$  would not be all  $z_{i,j}$  pairs but rather only features corresponding to valid edges of the graph, and we are only interested in invariances that preserve the graph structure, namely, the automorphisms of the graph. Thus, the desired invariance is that  $\sigma(\mathcal{F}(z)) = \mathcal{F}(\sigma(z))$  only for automorphisms of the graph. It is easy to see that Theorem 1 holds in this case, if one replaces the sum  $\sum_{j \neq i}$  with  $\sum_{j \in N(i)}$ , where  $N(i)$  are the neighbors of node  $i$  in the graph.

<sup>3</sup>This merely introduces another indexing step.

## 4. Deep Graph Prediction

Theorem 1 provides the general requirements for designing an architecture for structured prediction. For a given problem, one has to choose a specific architecture and parameterization for  $\alpha$ ,  $\phi$ ,  $\rho$ .

For instance, it is interesting to consider how an algorithm like belief propagation (BP) can be implemented in our framework. Following the proof of Theorem 1, one would use  $\phi$ ,  $\alpha$  to aggregate features, and then  $\rho$  would apply BP to these features. Our architecture is of course more general by construction. For example, it could use  $\phi$  and  $\alpha$  to “sketch” the input graph, such that labeling can be performed on a reduced representation.

We now survey certain architectures consistent with Theorem 1 and discuss their expressive power.

**Introducing Attention.** Attention is a powerful architectural component in deep learning (Bahdanau et al., 2015), but most inference algorithms do not use attention. We now show how attention can be introduced in our framework.

Intuitively, attention means that instead of aggregating features of neighbors, a node  $i$  weighs neighbors based on their relevance. For example, the label of an entity in an image may depend more strongly on entities that are spatially closer. We now implement attention for the architecture of Eq. 3. Formally, we learn attention weights for the neighbors  $j$  of a node  $i$ , which scale the features  $z_{i,j}$  of that neighbor. We can also learn different attention weights for individual features of each neighbor in a similar way.

Let  $w_{i,j} \in \mathbb{R}$  be an attention mask specifying the weight that node  $i$  gives to node  $j$ :

$$w_{i,j}(z_i, z_{i,j}, z_j) = e^{\beta(z_i, z_{i,j}, z_j)} / \sum_t e^{\beta(z_i, z_{i,t}, z_t)}, \quad (6)$$

where  $\beta$  can be any scalar-valued function of its arguments (e.g., a dot product of  $z_i$  and  $z_j$  as in standard attention models). To introduce attention we wish  $\alpha \in \mathbb{R}^e$  to have the form of weighting  $w_{i,j}$  over neighboring feature vectors  $z_{i,j}$ , namely,  $\alpha = \sum_{j \neq i} w_{i,j} z_{i,j}$ .

To achieve this form we extend  $\phi$  by a single entry, defining  $\phi \in \mathbb{R}^{e+1}$  (namely we set  $L = e+1$ ) as  $\phi_{1:e}(z_i, z_{i,j}, z_j) = e^{\beta(z_i, z_{i,j}, z_j)} z_{i,j}$  (here  $\phi_{1:e}$  are the first  $e$  elements of  $\phi$ ) and  $\phi_{e+1}(z_i, z_{i,j}, z_j) = e^{\beta(z_i, z_{i,j}, z_j)}$ . We keep the definition of  $s_i = \sum_{j \neq i} \phi(z_i, z_{i,j}, z_j)$ . Next, we define  $\alpha = \frac{s_{i,1:e}}{s_{i,e+1}}$  and substitute  $s_i$  and  $\phi$  to obtain the desired form as attention weights  $w_{i,j}$  over neighboring feature vectors  $z_{i,j}$ :

$$\alpha(z_i, s_i) = \frac{s_{i,1:e}}{s_{i,e+1}} = \frac{\sum_{j \neq i} e^{\beta(z_i, z_{i,j}, z_j)} z_{i,j}}{\sum_{j \neq i} e^{\beta(z_i, z_{i,j}, z_j)}} = \sum_{j \neq i} w_{i,j} z_{i,j}$$

A similar approach can be applied over  $\alpha$  and  $\rho$  to model attention over the outputs of  $\alpha$  as well (graph nodes).

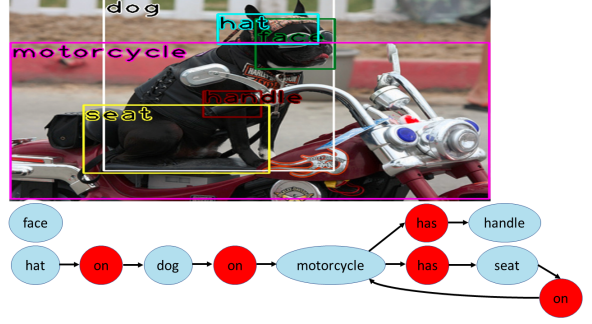


Figure 4. An image (top) and its scene graph (bottom) from the Visual Genome dataset (Krishna et al., 2017). The scene graph captures the entities in the image (nodes, blue circles) and their pairwise relations (edges, red circles). Example relationships in this graph include:  $\langle \text{hat, on, dog} \rangle$  and  $\langle \text{dog, on, motorcycle} \rangle$ .

**Using RNNs as Components.** Theorem 1 allows arbitrary functions for  $\phi$ ,  $\alpha$  and  $\rho$ , except for their input dimensionality. Specifically, these functions can involve highly expressive recursive computation, simulate existing message passing algorithms, and new algorithms that are learned from data. This can of course be extended to more elaborate structures like LSTMs (Hochreiter & Schmidhuber, 1997) and Neural Turing Machines (Graves et al., 2014), which we leave for future work.

Theorem 1 suggests that any function in the form of  $\mathcal{F}$  is graph permutation invariant. It is easy to show that composing two functions that are GPI, is also GPI. Therefore, we can run  $\mathcal{F}$  iteratively by providing the output of one step of  $\mathcal{F}$  as part of the input to the next step and maintain graph-permutation invariance. This results in a recurrent architecture, which we will employ in the next section to obtain state-of-the-art performance on scene graph prediction.

## 5. Application - Scene Graph Classification

We demonstrate the benefits of our axiomatic approach in the task of inferring scene graphs from images. In this problem, the input is an image annotated with a set of rectangles that bound entities in the image, known as *bounding boxes*. The goal is to label each bounding box with the correct entity category, and every pair of entities with their relation, such that they form a coherent graph, known as a *scene graph*. In a scene graph, nodes correspond to bounding boxes labeled with the entity category and edges correspond to relations among entities, which could be spatial (“on”) or functional (“wearing”). Thus, in an image with 5 bounding boxes there are  $5 + 5 \times 4 = 25$  output variables.

This concept is illustrated in Figure 4, showing an image of a dog on a motorcycle (top) and the corresponding scene

graph below. The pink box in the image is labeled “*motorcycle*” and the white box is labeled “*dog*”. These two boxes correspond to two nodes (light blue circles in Figure 4 bottom), and their relation “*on*” corresponds to an edge (red circle labeled “*on*”). While scene graphs are typically very sparse, one can view a scene graph as complete if each pair of unrelated entities is connected by a ‘null’ edge. A scene graph can be represented as a collection of triplets, each with a relation and two entities, like  $\langle \textit{dog}, \textit{on}, \textit{motorcycle} \rangle$ .

### 5.1. Model

Our model has two components: A *Label Predictor (LP)* that takes as input an image with bounding boxes and outputs a distribution over labels for each entity and relation. Then, a *Scene Graph Predictor (SGP)* that takes all label distributions and predicts more consistent label distributions jointly for all entities and relations.

**Label Prediction.** The LP module (Figure 5) receives an input image  $x$  and a set of bounding boxes  $bb_1, \dots, bb_n$ , corresponding to image entities (as in Figure 4). LP outputs a set of entity label probabilities  $p(y_i^{\text{ent}} | bb_i)$  for each box  $i$  from a pre-defined set of candidate entity labels  $\mathcal{P}$  and a set of relation probabilities  $p(y_{i,j}^{\text{rel}} | bb_i, bb_j)$  from another pre-defined set of relation labels  $\mathcal{R}$ . These unary and pairwise potentials are later fed to the SGP module.

To predict entity labels, we used RESNET50 (He et al., 2016a;b), taking as input a patch cropped from the full image according to the  $i^{\text{th}}$  bounding box (Figure 5). We used a second RESNET50 to predict relations, using a 5-channel tensor input: three channels for the RGB image, and two channels for binary masks for the subject entity and object entity bounding boxes (Figure 5). The image patch provided to this network was cropped such that it covers both the subject entity and the object entity. Providing the two binary masks breaks the symmetry of the subject entity and object entity and allow the network to discriminate between triplets like  $\langle \textit{man}, \textit{wearing}, \textit{shirt} \rangle$  and  $\langle \textit{shirt}, \textit{on}, \textit{man} \rangle$ .

**Scene Graph Prediction.** While the LP module described above is trivially GPI, because the output variables  $y_i^{\text{ent}}, y_{i,j}^{\text{rel}}$  are predicted independently, constructing a GPI architecture for a *Scene Graph Predictor* is harder. We now outline this construction. Entity classification in this module is GPI following Theorem 1, where  $z_i$  are features for every bounding box and  $z_{i,j}$  are features for box pairs. To classify relations, we added a function  $\rho_{\text{relation}}$  that reuses the GPI representation created during entity classification. Because the input to  $\rho_{\text{relation}}$  is a GPI representation, it is easy to show that our entire network is GPI.

Let  $z_i$  be the concatenation of  $z_i^{\text{features}}$  and  $z_i^{\text{spatial}}$ . Where  $z_i^{\text{features}}$  is the current label probability for entity  $i$  (logits

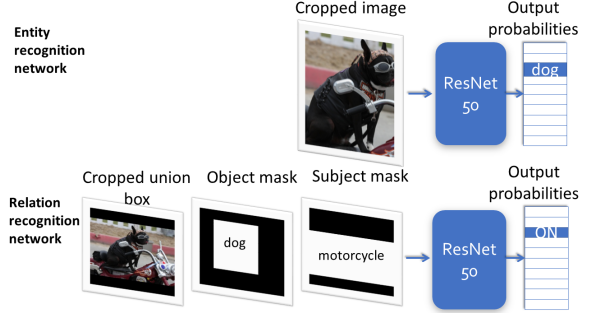


Figure 5. **The Label Predictor.** (a) **Entity recognition network:** A network takes an image patch cropped based on a bounding box, and outputs classification probabilities per label. (b) **Relation recognition network:** A network takes an input tensor, containing the RGB image in the first 3 channels, and two binary masks for the subject and object entities in the remaining two channels.

before the final softmax layer) and  $z_i^{\text{spatial}}$  is  $i$ 's bounding box given as a  $(x, y, \text{width}, \text{height})$ . In addition, for  $z_{i,j}$ , we used the confidences for relation  $i, j$  (logits before the final softmax layer). In each step of SGP we apply the function  $\mathcal{F}$ , which receives all entity features  $z_i$  and all relation features  $z_{i,j}$ , and output updated confidences for entities and relations. Because composing GPI functions is GPI, our SGP module is GPI. We now describe our implementation of the three components of  $\mathcal{F}$ :  $\phi$ ,  $\alpha$  and  $\rho$ .

(1)  $\phi$  is a network with two FC-layers. It receives (a) subject features  $z_i$  (b) relations features  $z_{i,j}$  (c) entity features  $z_j$  and outputs a vector of size 500. Next, for each entity  $i$ , we aggregate  $\phi(z_i, z_{i,j}, z_j)$  into  $s_i$  using the attention mechanism described in Section 4. To calculate the weights  $w_{i,j}$ , we implement  $\beta(\cdot)$  (Eq. 6) with a FC layer that receives the same input as  $\phi$  and outputs a scalar.

(2)  $\alpha$  is a two FC-layer network, receiving entity features  $z_i$  and context features  $s_i$ . The outputs of  $\alpha$  are aggregated with a similar attention mechanism over entities, resulting in a vector  $g \in \mathbb{R}^{500}$  representing the entire graph.

(3)  $\rho$ , consists of  $\rho_{\text{entity}}$ , which classifies entities, and  $\rho_{\text{relation}}$ , which classifies relations.  $\rho_{\text{entity}}$  is a three FC-layer network of size 500. It receives  $z_i, s_i$  and  $g$  as input, and outputs a vector  $q_i$  with one scalar per entity class. Unlike Theorem 1, we allow  $\rho$  direct access to  $s_i$ , which maintains the GPI property, and improved learning in practice. The final output confidence is a linear interpolation of the current confidence  $z_i^{\text{features}}$  and the new confidence  $q_i$ , controlled by a learned forget gate, i.e., the output is  $q_i + \text{forget} \cdot z_i^{\text{features}}$ .  $\rho_{\text{relation}}$ , the relation classifier, is analogous to the entity classifier, receiving as input  $z_i, z_j$ , the relation features  $z_{i,j}$ , and the graph representation  $g$ .

We also explored concatenating word embeddings of the most probable entity class to  $z_i$ . Word vectors were learned with GLOVE (Pennington et al., 2014) from the ground-truth captions of Visual Genome (Krishna et al., 2017).

## 5.2. Experimental Setup

**Dataset.** We evaluated our approach on the Visual Genome (VG) dataset (Krishna et al., 2017). VG consists of 108,077 images annotated with bounding boxes, entities and relations. Distribution over entity classes and relations is long-tailed with a total of 75,729 unique entity classes and 40,480 unique relations. To allow apple-to-apple comparison with previous studies of this dataset (Xu et al., 2017; Newell & Deng, 2017; Zellers et al., 2017), we used the same preprocessed data, including the train and test splits, as provided by (Xu et al., 2017). This dataset had on average 12 entities and 7 relations per image. For evaluation, we used the same 150 entity categories and 50 relations as in (Xu et al., 2017; Newell & Deng, 2017; Zellers et al., 2017). To tune hyper-parameters, we also split the training data into two by randomly selecting 5K examples, resulting in a final 70K/5K/32K split for train/validation/test sets.

**Training Procedure.** We trained all networks using Adam (Kingma & Ba, 2014); Input images were resized to 224x224 to conform with the RESNET architecture. We first trained the LP module, and then trained the SGP module using the best LP model.

In what follows, all the particular chosen values were tuned on the validation set. For LP, we trained the relation network with cross-entropy loss and a positive-to-negative ratio of 1:3 (where ‘positive’ refers to a labeled relation and ‘negative’ to unlabeled), and performed early-stopping after 90 epochs. We chose a batch size of 64, and also used data augmentation techniques such as translation and rotation to further improve the results. The loss function for the SGP was the sum of cross entropy losses over all entities and relations in the image. In the loss, we penalized entities 4 times more strongly than relations, and penalized negative relations 10 times more weakly than positive relations. We used batch size 100 and early-stopped after 120 epochs. The recurrent application of  $\mathcal{F}$  was performed for 2 steps.

**Evaluation.** Xu et al. (2017) defined three different sub-tasks when inferring scene graphs, and we focus on two: (1) **SGCls**: Given ground-truth bounding boxes for entities, predict all entity categories and relations categories. (2) **PredCls**: Given bounding boxes annotated with entity labels, predict all relations. Following (Lu et al., 2016), we used Recall@ $K$  as the evaluation metric. It measures the fraction of correct ground-truth triplets that appear within the  $K$  most confident triplets proposed by the model.

Two evaluation protocols are used in the literature, which

differ by whether they enforce graph constraints over model predictions. The first protocol requires that the top- $K$  triplets assign one consistent class per entity and relation. This rules out putting more than one triplet for a pair of bounding boxes. It also rules out inconsistent assignment, like a bounding box that is labeled as one entity in one triplet, and as another entity in another triplet. The second evaluation protocol does not enforce any such constraints.

**Models and baselines.** We compare four variants of our GPI approach with the reported results of four baselines that are currently the state-of-the-art on various scene graph sub-tasks. All models use the same data split and pre-processing as (Xu et al., 2017):

1. (LU ET AL., 2016): This work leverages word embeddings to fine-tune the likelihood of predicted relations.
2. (XU ET AL., 2017): This model passes messages between entities and relations, and iteratively refines the feature map used for prediction.
3. (NEWELL & DENG, 2017). The PIXEL2GRAPH model uses associative embeddings (Newell et al., 2017) to produce a full graph from the image.
4. (ZELLERS ET AL., 2017) The NEURALMOTIF method encodes global context for capturing high-order motifs in scene graphs.
5. GPI: NO ATTENTION: Our GPI model, but with no attention mechanism. Instead, following Theorem 1, we simply sum the features.
6. GPI: NEIGHBORATTENTION: Our GPI model, using attention over neighbors as described in Section 5.1.
7. GPI: MULTIATTENTION: Our GPI model, except that we learn different attention weights per feature.
8. GPI: LINGUISTIC: Same as GPI: MULTIATTENTION but also concatenating the word embedding vector for the most probable entity label (see Sec. 5.1).

## 5.3. Results

Table 1 lists recall@50 and recall@100 for four variants of our approach compared with three baselines, evaluating with graph constraints. The GPI approach performs well, and LINGUISTIC outperforms all baselines for both PredCls and SGCls. Table 2 provides a similar comparison when evaluating without graph constraints; again LINGUISTIC performs best. More details in the supplemental material.

Figure 6 illustrates the model behavior. Predicting isolated labels with LP (column (c)) mislabels several entities, but these are corrected after joint prediction (column (d)). Column (e) shows that the system learned to attend more to nearby entities (the window and building are closer to the tree), and column (f) shows that stronger attention is learned for the classes bird, presumably because it is usually more informative than common classes like tree.

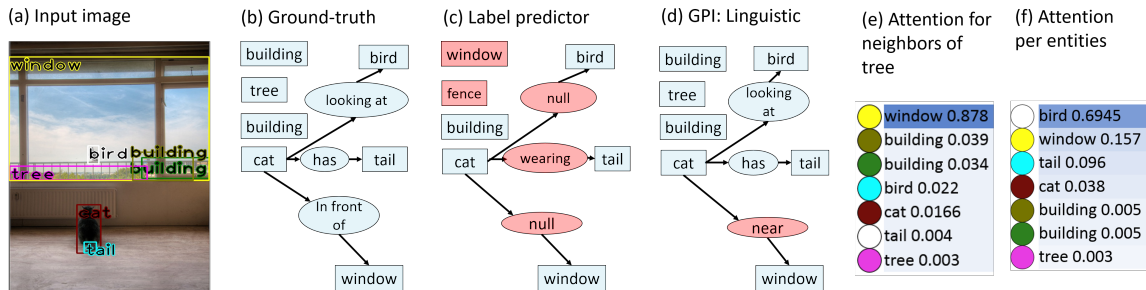


Figure 6. (a) An input image with bounding boxes from VG. (b) The ground-truth scene graph. (c) The LP fails to recognize some entities (*building* and *tree*) and relations (*in front of* instead of *looking at*). (d) GPI:LINGUISTIC fixes most incorrect LP predictions. (e) *Window* is the most significant neighbor of *Tree*. (f) The entity *bird* receives substantial attention, while *Tree* and *building* are less informative.

Table 1. Test set results for graph-constrained evaluation

	SGCLS		PREDCLS	
	R@50	R@100	R@50	R@100
(LU ET AL., 2016)	11.8	14.1	35.0	27.9
(XU ET AL., 2017)	21.7	24.4	44.8	53.0
NEURAL MOTIFS	31.3	32.1	65.8	68.0
NO ATTENTION	28.9	31.0	63.0	65.2
NEIGHBOR ATTEN.	30.6	32.4	63.7	66.5
MULTI ATTENTION	<b>32.3</b>	34.1	65.4	67.8
LINGUISTIC	32.1	<b>34.1</b>	<b>66.0</b>	<b>68.3</b>

Table 2. Test set results for unconstrained evaluation

	SGCLS		PREDCLS	
	R@50	R@100	R@50	R@100
PIXEL2GRAPH	26.5	30.0	68.0	75.2
NO ATTENTION	35.2	42.1	70.3	75.1
NEIGHBOR ATTEN.	37.6	43.2	73.7	79.2
MULTI ATTENTION	39.0	44.5	74.5	81.0
LINGUISTIC	<b>39.2</b>	<b>44.9</b>	<b>75.3</b>	<b>82.4</b>

## 6. Related Work

There has been significant recent interest in extending deep learning to structured prediction. Much of this work has been on semantic segmentation, where convolutional networks (Shelhamer et al., 2017) became a standard approach for obtaining “singleton scores” and various approaches were proposed for adding structure on top. Most of these approaches used variants of message passing algorithms, unrolled into a computation graph (Xu et al., 2017). Some studies parameterized parts of the message passing algorithm and learned its parameters (Lin et al., 2015). Recently, gradient descent has also been used for maximizing score functions (Belanger et al., 2017; Gygli et al., 2017).

An alternative approach for deep structured prediction is via greedy decoding, where one label is inferred at a time, based on previous labels. This has been popular in sequence-based applications like dependency parsing (Chen & Manning, 2014). These works rely on the sequential structure of the

Table 3. Recall@5 of PredCls for the 20-top relations ranked by their frequency, as in (Xu et al., 2017)

RELATION	LU ET AL. (2016)	XU ET AL. (2017)	LINGUISTIC
ON	<b>99.71</b>	99.25	99.4
HAS	98.03	97.25	<b>98.9</b>
IN	80.38	88.30	<b>96.2</b>
OF	82.47	96.75	<b>98.2</b>
WEARING	98.47	98.23	<b>99.5</b>
NEAR	85.16	<b>96.81</b>	95.0
WITH	31.85	88.10	<b>94.2</b>
ABOVE	49.19	79.73	<b>83.7</b>
HOLDING	61.50	80.67	<b>95.6</b>
BEHIND	79.35	<b>92.32</b>	90.6
UNDER	28.64	52.73	<b>83.2</b>
SITTING ON	31.74	50.17	<b>90.5</b>
IN FRONT OF	26.09	59.63	<b>74.7</b>
ATTACHED TO	8.45	29.58	<b>77.2</b>
AT	54.08	70.41	<b>81.1</b>
HANGING FROM	0.0	0.0	<b>74.7</b>
OVER	9.26	0.0	<b>54.9</b>
FOR	12.20	31.71	<b>43.4</b>
RIDING	72.43	89.72	<b>96.2</b>

input, where BiLSTMs can be effectively applied.

The concept of architectural invariance was recently proposed in DEEPSSETS (Zaheer et al., 2017). The invariance we consider is much less restrictive (i.e., we do not need to be invariant to all permutations of singleton and pairwise features, just those consistent with a graph re-labeling), and hence results in a substantially different set of architectures.

Extracting scene graphs from images provides a semantic representation that can later be used for reasoning, question answering, and image retrieval (Johnson et al., 2015; Lu et al., 2016; Raposo et al., 2017). It is at the forefront of machine vision research, integrating challenges like object detection, action recognition and detection of human-object interactions (Liao et al., 2016; Plummer et al., 2017).



## 7. Conclusion

We presented a deep learning approach to structured prediction, which constrains the architecture to be invariant to structurally identical inputs. As in score-based methods, our approach relies on pairwise features, capable of describing inter-label correlations, and thus inheriting the intuitive aspect of score-based approaches. However, instead of maximizing a score function (which leads to computationally-hard inference), we directly produce an output that is invariant to equivalent representations of the pairwise terms.

The axiomatic approach can be extended in many ways. For image labeling, geometric invariances (shift or rotation) may be desired. In other cases, invariance to feature permutations may be desirable. We leave the derivation of the corresponding architectures to future work. Finally, there may be cases where the invariant structure is unknown and should be discovered from data, which is related to work on lifting graphical models (Bui et al., 2013). It would be interesting to explore algorithms that discover and use such symmetries for deep structured prediction.

## References

- Bahdanau, D., Cho, K., and Bengio, Y. Neural machine translation by jointly learning to align and translate. In *International Conference on Learning Representations (ICLR)*, 2015.
- Belanger, David, Yang, Bishan, and McCallum, Andrew. End-to-end learning for structured prediction energy networks. In Precup, Doina and Teh, Yee Whye (eds.), *Proceedings of the 34th International Conference on Machine Learning*, volume 70, pp. 429–439. PMLR, 2017.
- Bui, Hung Hai, Huynh, Tuyen N., and Riedel, Sebastian. Automorphism groups of graphical models and lifted variational inference. In *Proceedings of the Twenty-Ninth Conference on Uncertainty in Artificial Intelligence*, UAI’13, pp. 132–141, Arlington, Virginia, United States, 2013. AUAI Press. URL <http://dl.acm.org/citation.cfm?id=3023638.3023652>.
- Chen, Danqi and Manning, Christopher. A fast and accurate dependency parser using neural networks. In *Proceedings of the 2014 conference on empirical methods in natural language processing (EMNLP)*, pp. 740–750, 2014.
- Chen, Liang Chieh, Papandreou, George, Kokkinos, Iasonas, Murphy, Kevin, and Yuille, Alan L. Semantic image segmentation with deep convolutional nets and fully connected CRFs. In *Proceedings of the Second International Conference on Learning Representations*, 2014.
- Chen, Liang Chieh, Schwing, Alexander G, Yuille, Alan L, and Urtasun, Raquel. Learning deep structured models. In *Proc. ICML*, 2015.
- Farabet, Clement, Couprie, Camille, Najman, Laurent, and LeCun, Yann. Learning hierarchical features for scene labeling. *IEEE transactions on pattern analysis and machine intelligence*, 35(8):1915–1929, 2013.
- Graves, Alex, Wayne, Greg, and Danihelka, Ivo. Neural Turing machines. *arXiv preprint arXiv:1410.5401*, 2014.
- Gygli, Michael, Norouzi, Mohammad, and Angelova, Anelia. Deep value networks learn to evaluate and iteratively refine structured outputs. In Precup, Doina and Teh, Yee Whye (eds.), *Proceedings of the 34th International Conference on Machine Learning*, volume 70 of *Proceedings of Machine Learning Research*, pp. 1341–1351, International Convention Centre, Sydney, Australia, 2017. PMLR.
- He, Kaiming, Zhang, Xiangyu, Ren, Shaoqing, and Sun, Jian. Deep residual learning for image recognition. In *2016 IEEE Conference on Computer Vision and Pattern Recognition, CVPR 2016, Las Vegas, NV, USA, June 27–30, 2016*, pp. 770–778, 2016a.
- He, Kaiming, Zhang, Xiangyu, Ren, Shaoqing, and Sun, Jian. Identity mappings in deep residual networks. In *ECCV*, volume 9908 of *Lecture Notes in Computer Science*, pp. 630–645. Springer, 2016b.
- Hochreiter, S. and Schmidhuber, J. Long short-term memory. *Neural Computation*, 9(8):1735–1780, 1997.
- Johnson, Justin, Krishna, Ranjay, Stark, Michael, Li, Li-Jia, Shamma, David A., Bernstein, Michael S., and Li, Fei-Fei. Image retrieval using scene graphs. In *IEEE Conference on Computer Vision and Pattern Recognition, CVPR 2015*, pp. 3668–3678, 2015.
- Kingma, Diederik P. and Ba, Jimmy. Adam: A method for stochastic optimization. *arXiv preprint arXiv: 1412.6980*, abs/1412.6980, 2014. URL <http://arxiv.org/abs/1412.6980>.
- Krishna, Ranjay, Zhu, Yuke, Groth, Oliver, Johnson, Justin, Hata, Kenji, Kravitz, Joshua, Chen, Stephanie, Kalantidis, Yannis, Li, Li-Jia, Shamma, David A, et al. Visual genome: Connecting language and vision using crowd-sourced dense image annotations. *International Journal of Computer Vision*, 123(1):32–73, 2017.
- Lafferty, J., McCallum, A., and Pereira, F. Conditional random fields: Probabilistic models for segmenting and labeling sequence data. In *Proceedings of the 18th International Conference on Machine Learning*, pp. 282–289, 2001.

- Liao, Wentong, Yang, Michael Ying, Ackermann, Hanno, and Rosenhahn, Bodo. On support relations and semantic scene graphs. *arXiv preprint arXiv:1609.05834*, 2016.
- Lin, Guosheng, Shen, Chunhua, Reid, Ian, and van den Hengel, Anton. Deeply learning the messages in message passing inference. In *Advances in Neural Information Processing Systems*, pp. 361–369, 2015.
- Lu, Cewu, Krishna, Ranjay, Bernstein, Michael S., and Li, Fei-Fei. Visual relationship detection with language priors. In *European Conference on Computer Vision*, pp. 852–869, 2016.
- Meshi, O., Sontag, D., Jaakkola, T., and Globerson, A. Learning efficiently with approximate inference via dual losses. In *Proceedings of the 27th International Conference on Machine Learning*, pp. 783–790, New York, NY, USA, 2010. ACM.
- Newell, Alejandro and Deng, Jia. Pixels to graphs by associative embedding. In *Advances in Neural Information Processing Systems 30 (to appear)*, pp. 1172–1180. Curran Associates, Inc., 2017.
- Newell, Alejandro, Huang, Zhiao, and Deng, Jia. Associative embedding: End-to-end learning for joint detection and grouping. In *Advances in Neural Information Processing Systems 30*, pp. 2274–2284. Curran Associates, Inc., 2017.
- Pei, Wenzhe, Ge, Tao, and Chang, Baobao. An effective neural network model for graph-based dependency parsing. In *Proceedings of the 53rd Annual Meeting of the Association for Computational Linguistics*, pp. 313–322, 2015.
- Pennington, Jeffrey, Socher, Richard, and Manning, Christopher D. Glove: Global vectors for word representation. In *Empirical Methods in Natural Language Processing (EMNLP)*, pp. 1532–1543, 2014. URL <http://www.aclweb.org/anthology/D14-1162>.
- Plummer, Bryan A., Mallya, Arun, Cervantes, Christopher M., Hockenmaier, Julia, and Lazebnik, Svetlana. Phrase localization and visual relationship detection with comprehensive image-language cues. In *ICCV*, 2017.
- Raposo, David, Santoro, Adam, Barrett, David, Pascanu, Razvan, Lillicrap, Timothy, and Battaglia, Peter. Discovering objects and their relations from entangled scene representations. *arXiv preprint arXiv:1702.05068*, 2017.
- Schwing, Alexander G and Urtasun, Raquel. Fully connected deep structured networks. *ArXiv e-prints*, 2015.
- Shelhamer, Evan, Long, Jonathan, and Darrell, Trevor. Fully convolutional networks for semantic segmentation. *IEEE Conference on Computer Vision and Pattern Recognition, CVPR 2015*, 39(4):640–651, 2017.
- Taskar, B., Guestrin, C., and Koller, D. Max margin Markov networks. In Thrun, S., Saul, L., and Schölkopf, B. (eds.), *Advances in Neural Information Processing Systems 16*, pp. 25–32. MIT Press, Cambridge, MA, 2004.
- Xu, D., Zhu, Y., Choy, C. B., and Fei-Fei, L. Scene Graph Generation by Iterative Message Passing. In *The IEEE Conference on Computer Vision and Pattern Recognition*. 2017.
- Zaheer, Manzil, Kottur, Satwik, Ravanbakhsh, Siamak, Poczos, Barnabas, Salakhutdinov, Ruslan R, and Smola, Alexander J. Deep sets. In Guyon, I., Luxburg, U. V., Bengio, S., Wallach, H., Fergus, R., Vishwanathan, S., and Garnett, R. (eds.), *Advances in Neural Information Processing Systems 30*, pp. 3394–3404. Curran Associates, Inc., 2017.
- Zellers, Rowan, Yatskar, Mark, Thomson, Sam, and Choi, Yejin. Neural motifs: Scene graph parsing with global context. *arXiv preprint arXiv:1711.06640*, abs/1711.06640, 2017. URL <http://arxiv.org/abs/1711.06640>.
- Zheng, Shuai, Jayasumana, Sadeep, Romera-Paredes, Bernardino, Vineet, Vibhav, Su, Zhizhong, Du, Dalong, Huang, Chang, and Torr, Philip HS. Conditional random fields as recurrent neural networks. In *Proceedings of the IEEE International Conference on Computer Vision*, pp. 1529–1537, 2015.